Journal of Alloys and Compounds 504S (2010) S247–S250

Contents lists available at ScienceDirect

Journal of Alloys and Compounds

journal homepage: www.elsevier.com/locate/jallcom

Isothermal crystallization in supercooled liquid state for $Ca_{50}Mg_{22.5}Cu_{27.5}$ metallic glass

D. Okai [a,*], Y. Shimizu [a], N. Hirano [a], T. Fukami [a], T. Yamasaki [a], A. Inoue [b]

[a] Department of Materials Science and Chemistry, Graduate School of Engineering, University of Hyogo, 2167 Shosha, Himeji 671-2280, Japan
[b] Institute of Materials Research, Tohoku University, 2-1-1 Katahira Aoba-ku, Sendai 980-8577, Japan

ARTICLE INFO

Article history:
Received 3 July 2009
Received in revised form 21 March 2010
Accepted 30 March 2010
Available online 7 April 2010

Keywords:
$Ca_{50}Mg_{22.5}Cu_{27.5}$
Metallic glass
Crystal growth
Diffusion process
Avrami exponent
Scaling law

ABSTRACT

The crystallization behavior of $Ca_{50}Mg_{22.5}Cu_{27.5}$ metallic glass in supercooled liquid has been examined using a technique of differential thermal analysis. Crystallization mechanism of the alloys during isothermal annealing in supercooled liquid was analyzed using the Johnson–Mehl–Avrami (JMA) equation. The experimental data of the isothermal crystallization was interpreted by the JMA model. The Avrami exponents for the ribbon and bulk alloys are 2.5 ± 0.5 and 2.3 ± 0.3, respectively. Both values of the Avrami exponent suggested that the crystal growth is controlled by a long-range diffusion process. The scaling law for crystallization of the alloys was also examined.

1. Introduction

Metallic glasses with a supercooled liquid have been fabricated for Mg–Ce–Ni [1], Al–La–Ni [2], Zr–Al–Ni [3] systems etc. The supercooled liquid state, which is a metastable state, changes finally into a stable crystalline structure. This transition is due to the lower energy level of crystalline state than that of supercooled liquid state below the melting temperature (T_m). For improving the stability of supercooled liquid state for metallic glasses, it is important to clear the crystallization mechanism in supercooled liquid state for metallic glasses. The time dependences of crystal nucleation and growth in supercooled liquid state for the metallic glasses have been analyzed from experimental data of differential thermal analysis (DTA) or differential scanning calorimetry (DSC) using Johnson–Mehl–Avrami (JMA) equation [4–9]. It has been reported that the crystallization mechanism for $Zr_{65}Cu_{27.5}Al_{7.5}$, $Pd_{42.5}Cu_{30}Ni_{7.5}P_{20}$ and $Mg_{65}Cu_{25}Y_{10}$ metallic glasses depends on temperature [4,5,9]. These results disagree with those expected from the JMA model.

Recently, novel metallic glasses of Ca–Mg–Cu alloys have been developed [10,11]. One of the thermal characteristics for Ca–Mg–Cu metallic glasses is that the alloy exhibits significantly lower glass transition temperature (T_g) than those of many metallic glasses. The T_g, crystallization temperature (T_x) and supercooled liquid region ($\Delta T_x = T_x - T_g$) for $Ca_{57}Mg_{19}Cu_{24}$ rod alloy with a diameter of 4 mm have been reported to be 404 K, 440 K and 36 K, respectively [10]. The Ca–Mg–Cu alloys with the essential characteristic have a potential for practical applications. The Ca–Mg–Cu alloys in the supercooled liquid state can be deformed to a desired shape using plastic molds. However, the crystallization of supercooled liquid arises for the deformation processes in supercooled liquid state. Hence, it is important to investigate the crystallization kinetics of the Ca–Mg–Cu alloys for industrial applications of the alloys.

In this paper, the crystallization mechanism of $Ca_{50}Mg_{22.5}Cu_{27.5}$ metallic glass in supercooled liquid region was investigated using an analyzing technique of the JMA model. The kinetics of crystallization for the ribbon and bulk alloys has been measured by a mean of DTA. The universality of crystal growth for crystallization in supercooled liquid for metallic glasses also was evaluated.

2. Experimental procedures

A master-alloy ingot of $Ca_{50}Mg_{22.5}Cu_{27.5}$ was prepared from pure Ca, Mg and Cu metals by an induction melting method in an argon atmosphere. The $Ca_{50}Mg_{22.5}Cu_{27.5}$ ribbon and bulk metallic glasses were fabricated by melt spinning and copper-mold casting methods in an argon gas atmosphere, respectively. The bulk metallic glass fabricated is a plate of 10 mm width and 4 mm thickness. The amorphous structure of the samples was examined by X-ray diffraction with Cu Kα radiation. Temperature and time dependences of exothermic for crystallization of the specimens during isothermal annealing were measured using a

* Corresponding author. Tel.: +81 79 267 4910; fax: +81 79 267 4910.
E-mail address: okai@eng.u-hyougo.ac.jp (D. Okai).

0925-8388/$ – see front matter © 2010 Elsevier B.V. All rights reserved.
doi:10.1016/j.jallcom.2010.03.225

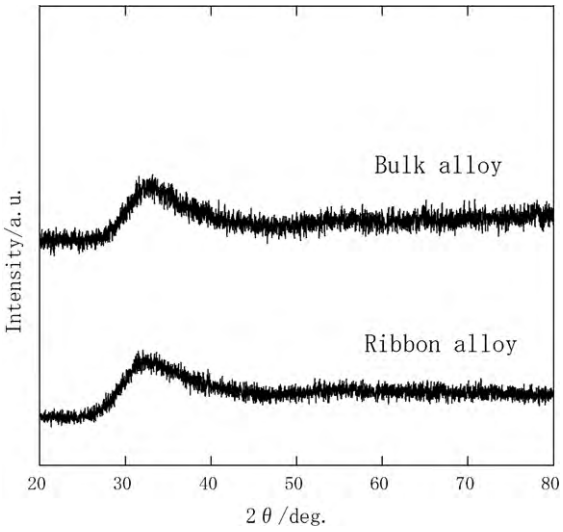

Fig. 1. X-ray diffraction patterns for the $Ca_{50}Mg_{22.5}Cu_{27.5}$ ribbon and bulk metallic glasses.

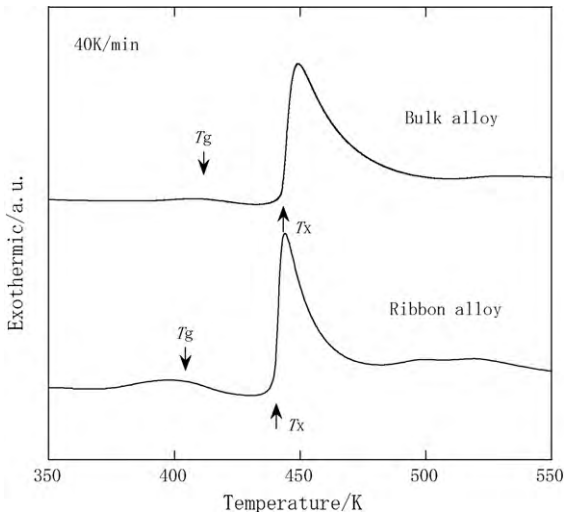

Fig. 2. DTA curves for the $Ca_{50}Mg_{22.5}Cu_{27.5}$ ribbon and bulk metallic glasses.

DTA of TG8120 model produced by Rigaku Co. Ltd. The isothermal DTA measurements were carried out at various constant temperatures below T_x for specimens in an argon atmosphere with a heating rate of 40 K/min. The fraction of crystallization at a time t after crystals start growing, $y(t)$, was determined by a ratio $A(t)/A(\infty)$, where $A(t)$ is the area under the exothermic peak up to time t and $A(\infty)$ is the total area of the peak. The area was estimated by measuring the ordinate at closely spaced values of t and using the Simpson type integration.

The $y(t)$ for JMA model is given by the following equation:

$$y(t) = 1 - \exp[1 - kt^N], \quad (1)$$

where k is a kinetic parameter depending temperature and N is the Avrami exponent relating to the mechanism of crystal nucleation and growth [12–15]. Here, the Eq. (1) is described under some assumptions. The crystallization mechanism of the alloys can be estimated from the Avrami exponent of the JMA formula. In case of a short-range diffusion for 3-dimensional, the N is expected to be 3 for latent germ nuclei or 4 for constant nucleation rate of germ nuclei. In case of a long-range diffusion for 3-dimensional system, the N is 1.5 for latent germ nuclei or 2.5 for constant nucleation rate of germ nuclei.

3. Results and discussion

Fig. 1 shows the X-ray diffraction patterns for the $Ca_{50}Mg_{22.5}Cu_{27.5}$ ribbon and bulk metallic glasses. The broadened diffused-diffraction peak for the alloys is the typical characterization of amorphous structure. Fig. 2 shows the DTA curves for the $Ca_{50}Mg_{22.5}Cu_{27.5}$ ribbon and bulk metallic glasses. The thermal stability associated with crystallization for the samples was measured by DTA under a flowing argon atmosphere with a heating rate of 40 K/min. The thermal parameters of $Ca_{50}Mg_{22.5}Cu_{27.5}$ metallic glass are the $T_g = 404$ K, $T_x = 440$ K and $\Delta T_x = 36$ K for the ribbon alloy, and the $T_g = 412$ K, $T_x = 443$ K and $\Delta T_x = 31$ K for the bulk alloy.

Fig. 3 shows the isothermal DTA plots at various annealing temperatures for the $Ca_{50}Mg_{22.5}Cu_{27.5}$ metallic glasses in the supercooled liquid state. The peak height of DTA curves decrease and their width becomes wider with decreasing temperature. The partial crystallization $y(t)$ was estimated from the data shown in Fig. 3. The X-ray diffraction pattern (XRD) of samples after DTA measurements for the $Ca_{50}Mg_{22.5}Cu_{27.5}$ alloys indicated that the crystallized alloys contain $CaMg_2$, CaCu and unknown phases.

Fig. 4 shows the $\ln[-\ln\{1 - y(t)\}]$ vs. $\ln t$ (the JMA plots) at several temperatures for the $Ca_{50}Mg_{22.5}Cu_{27.5}$ metallic glasses in the range of $0.1 < y(t) < 0.9$. The value of N can be estimated from the slope of the JMA plots for each temperature. The N values for the ribbon and bulk alloys was obtained to be 2.5 ± 0.5 and 2.3 ± 0.3, respectively. There was no difference in N value between the ribbon and bulk specimens. The scatter of the Avrami exponents for the ribbon alloy was slightly larger than that of the bulk alloy. The N values for the alloys indicated that the crystal growth is controlled by long-range order diffusion in 3-dimensional system with latent germ nuclei. The results of XRD for specimens after DTA measurements also suggest that the crystal growth is controlled by long-range order diffusion. In many cases, transformation of structure, which is thermal equilibrium, occur without the change of mean chemical composition between the old and new phases. Therefore, in this case, the growth of new phase is controlled by a short-range diffusion of chemical elements. The crystallization mechanism of Zr-based metallic glasses, which have the composition similar to $Zr_2(Cu, Al)$ precipitates by isothermal annealing, has been reported to be ruled by short-range diffusion processes for $Zr_{50}Al_{10}Cu_{40}$ and $Zr_{65}Al_{10}Cu_{25}$ alloys [7]. In the case that the chemical composition of new phase differs from that of the old phase, the diffusion process is controlled by a long-range diffusion process. In this work, the results of XRD indicated that the chemical composition between the old and new phases is different for the $Ca_{50}Mg_{22.5}Cu_{27.5}$ alloy.

Fig. 5 shows the time-scaling of $y(t)$ normalized by $t_{1/2}$ for the $Ca_{50}Mg_{22.5}Cu_{27.5}$ metallic glasses. The scaling law relative to a universality of crystallization for the $Ca_{50}Mg_{22.5}Cu_{27.5}$ alloys was investigated from data shown in Fig. 2. The half of the completion time of crystallization, $t_{1/2}$ is defined as the scaling time. The scaling curves in final stage of the crystal growth for both of the alloy were deviated each other. The scatter of the scaling curves may arise from the variation of diffusion velocity with the time during the crystallization. The crystal can grow largely enough without mutual impediment among growing crystals in the first stage of crystallization. On the other hand, the each crystal is impeded to grow by others in the final stage of crystal growth. The scaling of curves for $Ca_{50}Mg_{22.5}Cu_{27.5}$ alloy is not good compared with $Zr_{55}Cu_{30}Al_{10}Ni_5$ and $Zr_{65}Al_{10}Cu_{25}$ metallic glasses [6,7]. The scaling curves have almost collapsed a single curve for the two Zr-based alloys. To clear the universality of crystallization for $Ca_{50}Mg_{22.5}Cu_{27.5}$ alloy, it may be needed furthermore experiments.

The activation energy (E_a) for the alloys was estimated from plots of $\ln t_{1/2}$ vs. $1/T$. The E_a values for the ribbon and bulk alloys are 177 kJ/mol and 205 kJ/mol, respectively. It has been reported that the E_a for $Mg_{65}Cu_{25}Y_{10}$ metallic glass is 139 kJ/mol [9]. The E_a

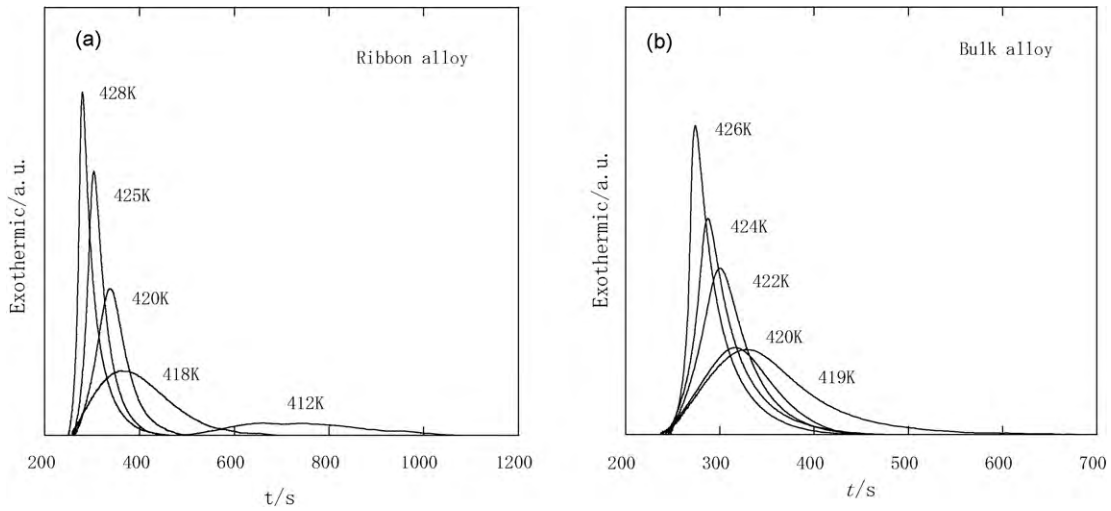

Fig. 3. Isothermal DTA plots at various annealing temperatures for the $Ca_{50}Mg_{22.5}Cu_{27.5}$ alloys in supercooled liquid state. (a) $Ca_{50}Mg_{22.5}Cu_{27.5}$ ribbon alloy and (b) $Ca_{50}Mg_{22.5}Cu_{27.5}$ bulk alloy.

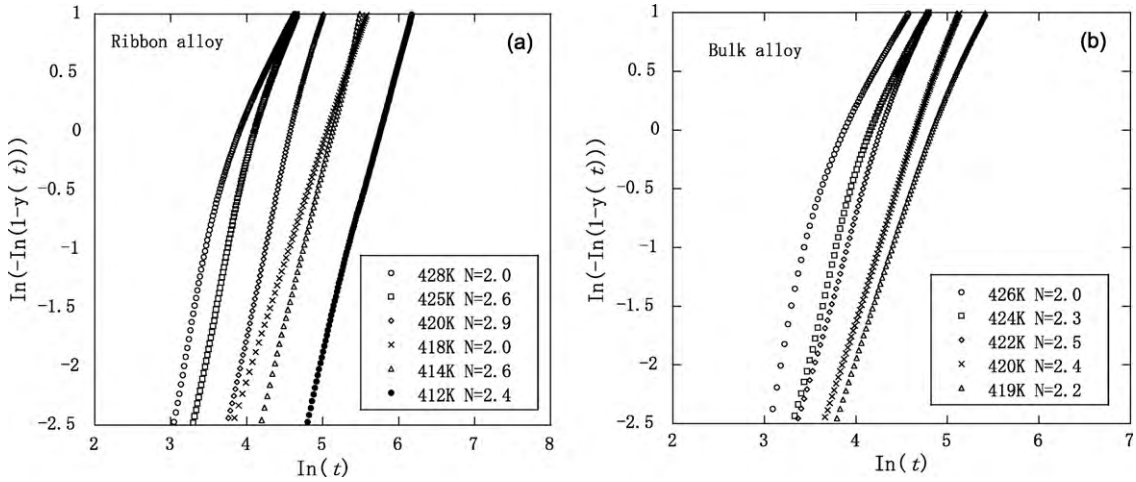

Fig. 4. $\ln[-\ln\{1-y(t)\}]$ vs. $\ln t$ (the JMA plots) at several temperatures for the $Ca_{50}Mg_{22.5}Cu_{27.5}$ ribbon and bulk metallic glasses. (a) $Ca_{50}Mg_{22.5}Cu_{27.5}$ ribbon alloy and (b) $Ca_{50}Mg_{22.5}Cu_{27.5}$ bulk alloy.

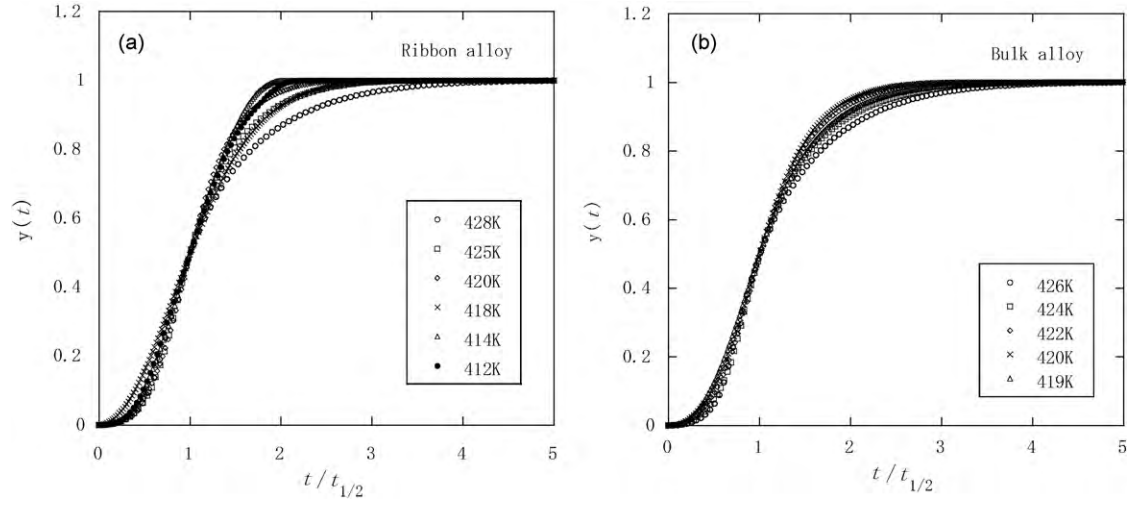

Fig. 5. Time-scaling of $y(t)$ normalized by $t_{1/2}$ for the $Ca_{50}Mg_{22.5}Cu_{27.5}$ ribbon and bulk metallic glasses. The $t_{1/2}$ is defined as the half of the completion time of crystallization. (a) $Ca_{50}Mg_{22.5}Cu_{27.5}$ ribbon alloy and (b) $Ca_{50}Mg_{22.5}Cu_{27.5}$ bulk alloy.

for $Ca_{50}Mg_{22.5}Cu_{27.5}$ alloys is found out to be larger than that for the $Mg_{65}Cu_{25}Y_{10}$ alloy.

4. Conclusion

The isothermal crystallization of $Ca_{50}Mg_{22.5}Cu_{27.5}$ metallic glass in supercooled liquid has been investigated using a technique of differential thermal analysis. The crystallization mechanism of the $Ca_{50}Mg_{22.5}Cu_{27.5}$ ribbon and bulk alloys in supercooled liquid was analyzed using the Johnson–Mehl–Avrami (JMA) formula. The Avrami exponents for the ribbon and bulk alloys are 2.5 ± 0.5 and 2.3 ± 0.3, respectively. The experimental Avrami exponents were agreement with that predicted by the JMA model. The values of Avrami exponent for the alloys suggested that the crystal growth is controlled by a long-range diffusion process. The activation energy for crystallization of the $Ca_{50}Mg_{22.5}Cu_{27.5}$ ribbon and bulk metallic glasses was estimated by the Arrhenius plots of $\ln t_{1/2}$ vs. $1/T$.

References

[1] A. Inoue, K. Ohtera, K. Kita, T. Masumoto, Jpn. J. Appl. Phys. 27 (1988) L2248–L2251.
[2] A. Inoue, T. Zhang, T. Masumoto, Mater. Trans. JIM 30 (1989) 965–972.
[3] A. Inoue, T. Zhang, T. Masumoto, Mater. Trans. JIM 31 (1990) 177–183.
[4] D. Kawase, A.P. Tsai, A. Inoue, T. Masumoto, Appl. Phys. Lett. 62 (1993) 137–139.
[5] M. Qi, H.J. Fecht, Mater. Charact. 47 (2001) 215–218.
[6] T. Fukami, K. Okabe, D. Okai, T. Yamasaki, A. Inoue, Mater. Sci. Eng. B 111 (2004) 189–196.
[7] T. Fukami, H. Yamamoto, D. Okai, Y. Yokoyama, T. Yamasaki, A. Inoue, Mater. Sci. Eng. B 131 (2006) 1–8.
[8] Q. Chen, L. Liu, K.C. Chan, J. Alloys Compd. 419 (2006) 71–75.
[9] B. Gun, K.J. Laws, M. Ferry, J. Non-Cryst. Solids 352 (2006) 3887–3895.
[10] K. Amiya, A. Inoue, Mater. Trans. JIM 43 (2002) 81–84.
[11] O.N. Senkov, J.M. Scott, D.B. Miracle, J. Alloys Compd. 424 (2006) 394–399.
[12] M. Avrami, J. Chem. Phys. 7 (1939) 1103–1112.
[13] M. Avrami, J. Chem. Phys. 8 (1940) 212–224.
[14] M. Avrami, J. Chem. Phys. 9 (1941) 177–184.
[15] W. Johnson, R.F. Mehl, Met. Technol. (1938) 1089.